



Effect of Different Environmental Conditions on Durabilities of Polyester- and Vinylester-Based Glass-Fiber-Reinforced Polymer Pultruded Profiles

Shulan Yang*, Mingkun Chu, Fangyi Chen, Miaorui Fu, Yiwen Lv, Ziyi Xiao, Ningning Feng, Yang Song and Jiannan Li

Faculty of Civil and Architectural, Changzhou Institute of Technology, Changzhou, China

OPEN ACCESS

Edited by:

Jiaqing Wang,
Nanjing Forestry University, China

Reviewed by:

Francesco Ascione,
University of Salerno, Italy
Rui Miranda Guedes,
University of Porto, Portugal
Manickam Ramesh,
Kalaigaijankarunaidhi Institute of
Technology (KIT), India
Sharifah Shahnaz Syed Bakar,
Universiti Malaysia Perlis, Malaysia

*Correspondence:

Shulan Yang
yangsl@czu.cn

Specialty section:

This article was submitted to
Structural Materials,
a section of the journal
Frontiers in Materials

Received: 26 January 2022

Accepted: 14 March 2022

Published: 27 April 2022

Citation:

Yang S, Chu M, Chen F, Fu M, Lv Y,
Xiao Z, Feng N, Song Y and Li J (2022)
Effect of Different Environmental
Conditions on Durabilities of Polyester-
and Vinylester-Based Glass-Fiber-
Reinforced Polymer Pultruded Profiles.
Front. Mater. 9:862872.
doi: 10.3389/fmats.2022.862872

This paper presents the results of experimental investigations on the durability of glass-fiber-reinforced polymer (GFRP) pultruded profiles made of unsaturated polyester (UP) and vinylester (VE) resins commonly used in civil engineering. The water absorption, tensile properties, and microstructures of GFRP profiles exposed to several typical accelerated aging environments (e.g., deionized water, salt water, salt fog, and combined hygrothermal cycles) for 12 months were investigated. Moreover, a sustained loading factor was included in the test to reflect the behavior of the GFRP profiles in real structures. A normalization approach based on the controlled specimens was used to assess the effectiveness and relevance of the accelerated exposure. The results indicated that the maximum moisture absorption of both UP and VE GFRP profiles was immersed in deionized water, where the masses increased by 1.03 and 0.53%, respectively, leading to the maximum degradation of tensile strength (24.03%) of UP GFRP profile immersion in deionized water after 360 days of aging. However, the tensile modulus was more sensitive to high temperatures and has the maximum degradation (47.03%) after hygrothermal cycles. Moreover, VE GFRP profiles show superior humidity and temperature endurance. Furthermore, the sustained loading exacerbated the degradation of tensile properties slightly under the same conditions. Finally, by incorporating the cumulative damage caused by the sustained loading and a time-dependent factor into a residual strength model, a revised model was proposed to describe the tensile strength loss of pultruded UP GFRP profiles.

Keywords: glass fiber, polymer composites, durability, sustained loads, cumulative damage model, residual strength

INTRODUCTION

In recent years, the use of innovative materials has been promoted to address the limited durability of civil engineering structures made with traditional materials, such as steel and reinforced concrete, as well as their increasing rehabilitation costs (Dell'Anno and Lees, 2012; Qu et al., 2021). Among the new materials, glass-fiber-reinforced polymer (GFRP) composites play a particularly important role, especially for pultruded GFRP composites, because they can be tailor-made to suit the specific

purpose and be assembled at the scene quickly (Gribniak et al., 2021). Because most structures used in the outdoor environment are designed for a service life of at least 50 years, the composites should be exposed to different environments for a very long time. The erosion factors such as moisture absorption, changed temperature, chemical medium, and ultraviolet coupled with sustained loads under different environmental conditions caused color change and material peeling off in the surface, crack propagation in the matrix, and mechanical property degradation in the composite materials as time grows.

To date, numerous investigations have been concentrated on the effects of moisture absorption on the durability of fiber-reinforced polymer (FRP) composites (Nakada and Miyano, 2014). Starkova et al. (2021) found that 15-years long exposure of FRP bars in a humid environment resulted in a decrease of their interlaminar shear strength of 10–50%. In a test of natural fiber-reinforced polymer materials in different solutions for 180 days, a reduction in tensile strength and an increase in 8.5% weight had been reported by Ma et al. (2018). In a 28-day deionized water immersion test, Dell'Anno and Lees (2012) investigated the interlaminar shear performance of epoxy-based FRP composites. The reduction of interlaminar shear strength (ILSS) of epoxy-based FRP composites was about 43%, and it was reduced considerably upon immersion. They described that moisture creates a dual mechanism of stress relaxation–swelling–mechanical adhesion and breakdown of chemical bonds between the fiber and matrix at the interface.

The presence of sodium chloride salts in an aqueous exposure environment could affect the rate of water absorption, equilibrium moisture content, and mechanical properties of FRP composites. Based on data of 557 experiments on tensile strength and elastic modulus of GFRP and BFRP bars exposed to different harsh environments collected from the existing literature, Duo et al. (2021) discovered that the tensile strength of GFRP and BFRP bars had the best durability in salt solution. Similar results were reported in the paper of Fang et al. (2017). The flexural strength was reduced by 13.5 and 9.8% for GFRP composites after 6 months of aging in water and seawater, respectively. In contrast to these results, Chin et al. (1999) found that the equilibrium moisture content of epoxy-based GFRP composites in water and seawater was 1.42 and 1.79, respectively. In Vizentin's 12-month study (Vizentin and Vukelic, 2022), FRP composite samples submerged under sea exhibited dynamic and level declines in tensile strength compared with samples exposed to the room environment. Moreover, they invested in significant matrix morphological changes due to salt crystal formation and the impact of sea microorganisms embedding in the resin. It is noted that there are no clear trends of the effect of salt water on water absorption and mechanical properties of FRP composites. The results from these literature studies indicate that the presence of sodium chloride molecules in salt solution could either increase or decrease the rate of water absorption, equilibrium moisture content, and mechanical properties, depending on the specific chemistry of the resin matrix, cure cycle, cure state, exposure temperature, and so on.

Temperature may strongly affect the water absorption rate of FRP composites. It has been observed that a hygrothermal

environment, defined as a condition with combined moisture and elevated temperature, degrades the mechanical properties of FRP composites. Through the study of the effects of temperature and moisture, Scott and Lees. (2013) confirmed that the diffusivity at 60°C (~4.5) was approximately 1.5 times that at 20°C (~3%) with short-term tests on epoxy films subjected to water. In the research of Jiang et al. (2014) on glass/polyester composites, the specimens aged under 40°C water conditions (~0.890%) absorbed more than 6 times the moisture content compared to those under 20°C–50% aging conditions (~0.148%). Moreover, the tensile strength and modulus were influenced by the amount of water absorbed. Tu et al. (2019) investigated the hygrothermal aging behavior of thermoplastic composites. After 4 days of immersion in 85°C water, the effect of hygrothermal aging on the tensile properties of short glass fiber/PA66 composites was observed to be reduced by 49% in elastic modulus and 62% in tensile strength. Similar conclusions were drawn by Zeng et al. (2022), who found a significant decrease in tensile strength under a higher exposure temperature. In a 90 days study, Feng et al. (2014) found that increasing the temperature from 60 to 90°C resulted in a significant degradation in flexural properties.

According to previous research, the hygrothermal condition could be the main factor in the degradation of FRP composites. However, considering the combined effects of both the exposure environment and service loads is essential for determining the realistic service ability of FRP composites in civil engineering structures (Feng et al., 2014; Tu et al., 2019). Saini et al. (2016) discussed the combined effect of moisture and temperature on GFRP specimens with prestressed loading. The maximum reduction in strength was approximately 39% for the specimen exposed to a 55°C (the highest temperature among the varying hygrothermal conditions) water bath for 60 days. Liu et al. (2022) studied the durability behavior of FRP plates exposed to air, water spraying, and acid at 40°C with 25–65% f_u fatigue stresses. The test results show that the loads accelerated degradation of tensile strength, the internal pressure generated by the ingress liquid accelerates resin cracking, and fiber-matrix interface debonding. Kafodya et al. (2015) studied the durability behavior of CFRP plates exposed to water and seawater at room temperature with a sustained bending strain. The test results indicated tensile strength of specimens immersed in water and seawater decreased by approximately 18 and 13% at a 50% strain level, while the unstrained specimens decreased by 9 and 12%, respectively.

With respect to sustained loading, (Mancusi et al., 2013) the presence of salt, (Robert et al., 2012), and so on, the thermal and humid stresses on the fiber/matrix interface are likely to be magnified or restrained. In addition, according to a review of the investigations of the durability of FRP materials, experiments under accelerated conditions performed for the maximum durations are rarely longer than 12 months, and very few studies compared the performance of alternative resin systems. Therefore, understanding the changes in the material's strength with different matrix systems and consideration of the combined effects of these conditions are essential for a thorough understanding of the behavior of FRP composites applied in civil engineering.

This paper presents the results of experimental investigations of the water absorption, tensile properties, microstructure, and chemical structure of pultruded GFRP profiles made of two alternative resin systems—unsaturated polyester (UP) and vinylester (VE) resins—both composed of the same fiber architecture. Specimens from the two types of profiles were subjected to controlled environments for 12 months. The different conditions considered were as follows: 1) immersion in deionized water and salt water at room temperature, 2) exposure to salt fog cycles, 3) combined hygrothermal cycles, and 4) combined hygrothermal cycles with sustained loading. Furthermore, according to the theory of fracture mechanics, the effect of load was introduced to the accumulated damage, together with the environmental factors, and a time-dependent cumulative damage mode was put forward.

EXPERIMENTAL DETAILS

Materials and Processing

Two GFRP pultruded laminates were used in the experimental program. One was made of unsaturated polyester resin (UP profile) supplied by Jinling DSM Resins Co., Ltd., China, and the other was made of vinylester resin (VE profile) supplied by Shanghai Nobby Polymer Co., Ltd., China. Unidirectional E-glass fiber with a diameter of 24 μm , in the form of EDR480-T910, was manufactured by Mount Tai Glass Fiber Co., Ltd., China. The fiber volume fraction was approximately 60% for the compositions, of which approximately 50% is unidirectional roving and approximately 10% is bidirectional (0/90) woven fabrics. Pultruded laminates were processed by pulling E-glass continuous fibers with a silane sizing through a bath of a mixture of resin and the curing agent at 0.2 m min^{-1} by the producer at 110°C. Both TBPB and BPO have been used as curing agents, which represent 0.6 and 1.2% of the weight, respectively. The heat deflection temperature (HDT) for the resins measured by the producer is 110°C. In the heated molds, the temperature was set to 110°C to make the specimen surface obtain $\approx 95\%$ of complete polymerization inside the mold and eliminate the trapped water inside the GFRP specimens.

Environmental Conditions

The exposure environments were selected to evaluate the durability of GFRP profiles in typical environments of civil engineering applications. Specimens were exposed to the following environmental conditions:

Immersion in Deionized Water and Saltwater at Room Temperature

Specimens were immersed in deionized water and saltwater at the room environment (23°C, 65% RH). The saltwater solution comprised 3.5% by mass sodium chloride (3.5% NaCl) and deionized water. Both solutions were controlled at room temperature using enclosed glass conditioning chambers. In addition, an unexposed condition (storage in a room environment) was set to represent a control condition.

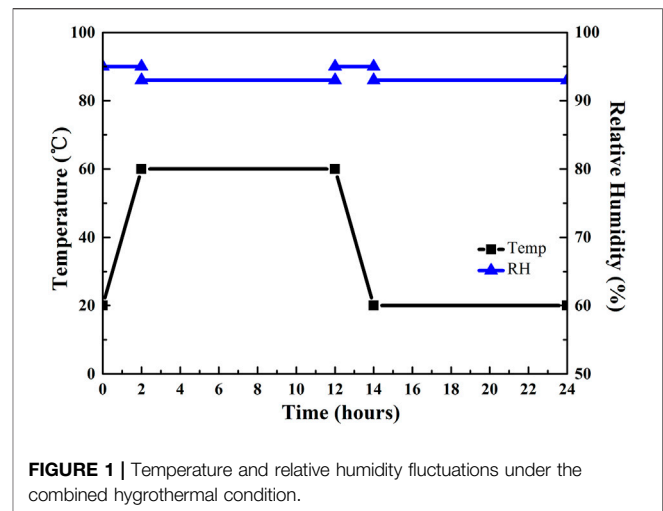


FIGURE 1 | Temperature and relative humidity fluctuations under the combined hygrothermal condition.

Exposure to Salt Fog Cycles

The accelerated cycles of salt fog were imposed in a chamber of YWX-100 provided by the Changzhou National Institute of Test Equipment with 5% NaCl solution (by mass). The fog cycles were programmed for 12 h of fogging, followed by 12 h of drying, and the test temperature was set at 35°C.

Combined Hygrothermal Cycles

Specimens were aged in the programmable temperature and humidity chamber provided by the Changzhou National Institute of Test Equipment for a different number of cycles. The overall duration of each combined hygrothermal cycle was 24 h, and it consisted of a combination of heating and cooling (20–60°C) at a combined humidity (93–95% RH), as shown in **Figure 1**.

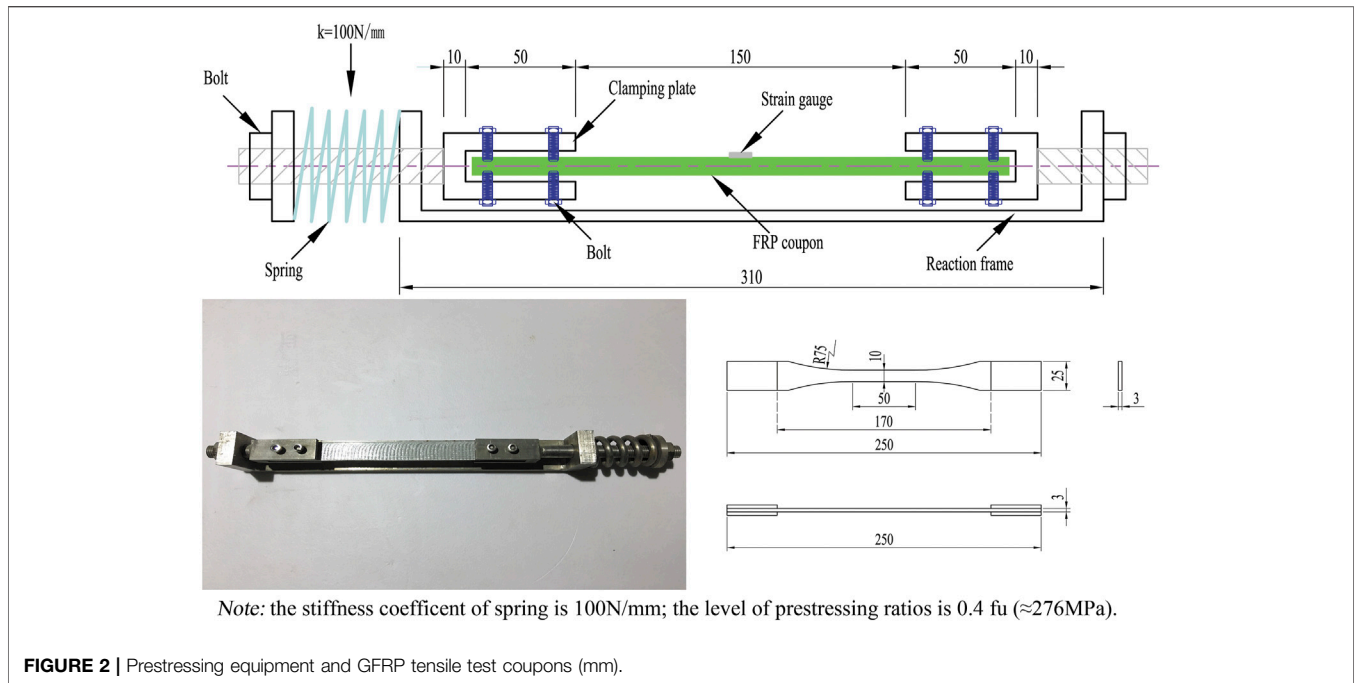
Combined Hygrothermal Cycles With Sustained Loading

A tensile fixture with a spring-reaction frame loading system, shown in **Figure 2**, was used to apply and maintain sustained loading on GFRP composites during combined hygrothermal cycles. The sustained loads applied to GFRP composites were 40% of the ultimate load, according to the existing guidelines (ACI 440.1R-06, 2006; ACI 440.2R-08, 2008). The force of sustained loading was determined by tightening the anchorage nut close to the spring and was controlled by a strain gauge placed on the coupon as Δx

$$\Delta x = \frac{\sigma_{ult} \cdot b \cdot h}{k} \quad (1)$$

where b is the width of the specimen, h is the thickness of the specimen, and k is the stiffness of the spring.

After 15, 30, 60, 90, 180, 270, and 360 days of aging, five specimens exposed to each type of condition were removed from the aging condition and tested to determine their mass changes, mechanical properties, and microscale performances.



Water Absorption Test

The specimen weight was recorded before and after aging as an effective approach to analyze the water absorption performance of pultruded GFRP profiles. The entire experiment was conducted in accordance with ASTM D5229/D5229M (2014). At regular time intervals, the specimens sized at 250 mm long, 25 mm wide, and 2.7 mm thick were removed, and both surfaces of the specimens were thoroughly cleaned with filter paper to remove excessive water and then kept in the room environment for 2 h. Then, five specimens for each condition were weighted and returned to the swelling medium. The experiment was continued until a constant sample weight was achieved. The moisture absorption M_t at any time can be calculated by Eq. 2

$$M_t = \left[\frac{m_t - m_i}{m_i} \right] \times 100\% \quad (2)$$

where m_i is the initial mass of the specimen prior to immersion and m_t is the mass of the specimen at immersion time t .

Tensile Test

The ultimate tensile strength and modulus of the composites were determined by standardized static tension tests in accordance with ASTM D3039/D3039M-14 (2014). The tensile tests were conducted after 15, 30, 60, 90, 180, 270, and 360 days of aging. At least five dumbbell-shaped specimens (see Figure 2) were tested using a universal testing machine (model CSS-44100) produced by the Changchun Research Institute, with a load cell having a capacity of 50 kN and a test speed of 2 mm/min. The tensile elongation of each specimen was monitored and recorded using a displacement meter that was placed at the middle of the specimen and set at zero at the beginning of the tensile test. All specimens were tested at 23°C and 65% RH.

Fourier Transform Infrared Spectroscopy

For the chemical characterization, Fourier transform infrared spectroscopy (FTIR) spectra of five specimens for each condition were studied in the 500–4,000 cm^{-1} range at a resolution of 4 cm^{-1} (32 scans) using a Nicolet-6700 spectrometer (produced by Thermo Fisher Scientific Co., Ltd., America). In all cases, specimens were ground into powders before the FTIR test for pultruded GFRP laminates, and the powders were ground into a dry KBr pellet.

Scanning Electron Microscopy

Scanning electron microscopy (SEM) observations and image analysis were performed using a QUANTA 200 instrument (Philips-FEI, Holland) to observe the microstructure of specimens before and after aging. Samples were taken from unconditioned specimens and specimens that were aged in deionized water, salt water, salt fog cycles, and combined hygrothermal cycles for 30 and 360 days. All specimens were cut from the surface and cross-section of samples and then coated with a gold film to improve their electrical conductivity before SEM observation.

RESULTS AND DISCUSSION

Moisture Absorption

Water final intake during the experimental program was shown in Table 1. Figures 3A,C illustrate the variations in the moisture absorption performances of UP and VE profiles with respect to the aging time. In the first 3 months, the increase in the moisture absorption of the UP profiles generated a progressive weight gain, approximately 80% of the total. Then, the weight gain saturated after a prolonged

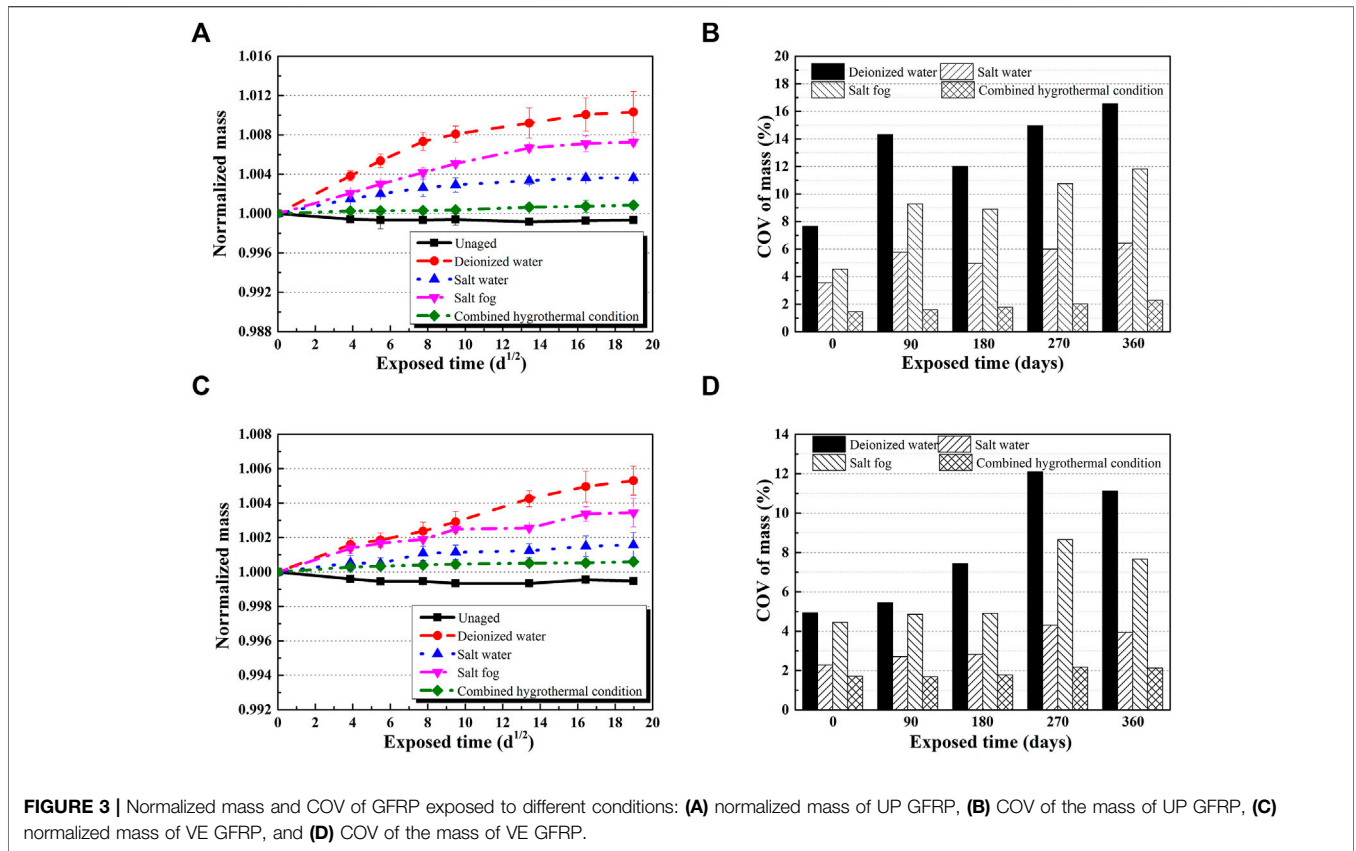


TABLE 1 | Water final intake during the experimental program.

Environment	Water uptake (g)	
	UP	VE
Deionized water	0.248	0.132
Salt water	0.087	0.400
Salt fog	0.177	0.085
Combined hygrothermal condition	0.022	0.015

time, somewhat in accordance with the classical Fick’s law (Figure 3A). However, the mass change curve of the VE profiles indicates multistage processes, with the declining region corresponding to the loss of styrene, as shown in Figure 3C. The GFRP profiles immersed in deionized water absorbed the most moisture (1.03% for UP-based resin and 0.53% VE-based resin) relative to those exposed in other aging environments, followed successively by the moisture in salt fog cycles (0.73% based on UP resin and 0.34% based on VE resin), in salt water (0.36% based on UP resin and 0.16% based on VE resin), and in combined hygrothermal cycles (0.09% based on UP resin and 0.06% based on VE resin). The results indicated that VE resin-based materials absorbed less moisture than UP-based materials, which was consistent with the results reported in the previous literature studies (Carra and Carvelli, 2014; Sousa et al., 2021). Figures 3B,D present the coefficient of

variation (COV) of GFRP in the test results showing a higher aging degree for exposed GFRP profiles than for the controlled profiles because the higher humidity and temperature provided by the exposure environment are conducive to the diffusion and absorption of moisture.

Thermal Analysis

Figure 4 shows the changes of glass-transition temperature with time in the aging process of UP and VE profiles under the hygrothermal cycle and heat coupled with sustained load. As can be seen in Figure 4A, T_g of UP profiles under the hygrothermal cycle and sustained loading increased from 87.14 to 88.97 and 91.17°C at 90 days, respectively, then gradually decreased, and gradually stabilized at 85.80 and 88.61°C after 270 days. The decreases were 3.17 and 2.56°C, respectively. As shown in Figure 4B, the T_g of the VE profiles still showed a trend of rising first and then decreasing. At 90 days, the T_g reached the maximum value of 100.14°C and then decreased and stabilized at 96°C, with a decrease of 4.14°C.

As a comprehensive reaction of various factors such as reflection, the existence of the sustained load, and deepening of the resin curing degree makes the maximum of T_g higher than that without load. Due to swelling of the composite material, the destruction of the van der Waals force, the enhancement of the hydrogen bond between molecules, and the hydrolysis reaction of the resin, the T_g decreased in a similar

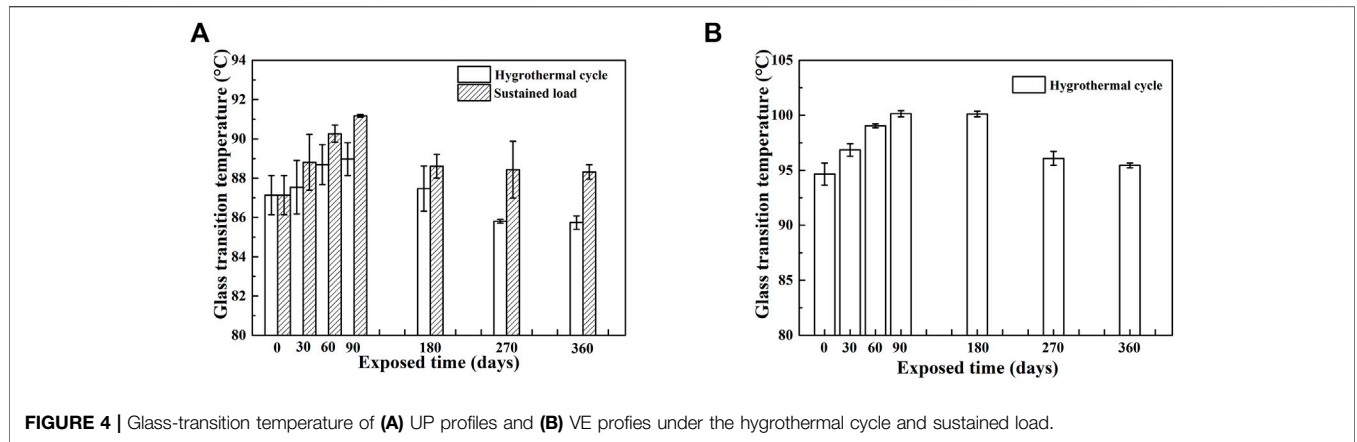
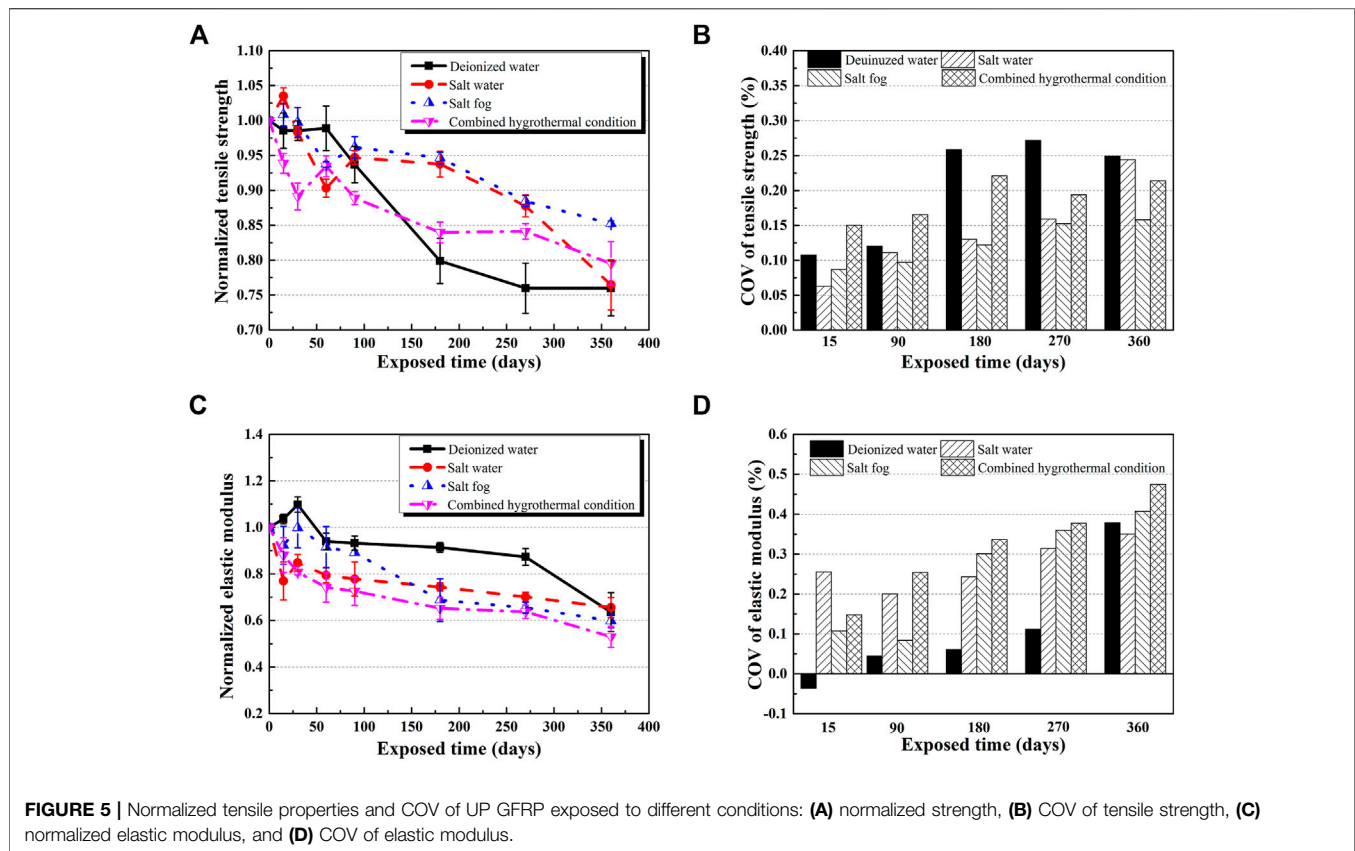


FIGURE 4 | Glass-transition temperature of (A) UP profiles and (B) VE profiles under the hydrothermal cycle and sustained load.

TABLE 2 | Results of tensile tests.

Types	Environment	Durations (day)	Tensile strength (MPa)			Strength retention (%)	Elastic modulus (GPa)			Modulus variation (%)
			Mean	SD	COV (%)		Mean	SD	COV (%)	
UP			Unexposed tensile strength = 503.512 (MPa); Unexposed elastic modulus = 9.871 (GPa)							
	Deionized water	15	496.265	59.98	12.09	98.56	10.221	-0.23	-2.25	-3.59
		90	471.794	64.60	13.69	93.70	9.209	0.49	5.33	6.77
		180	402.301	140.45	34.91	79.90	9.026	0.81	8.98	8.66
		360	382.529	126.99	33.20	75.97	6.271	3.42	54.54	36.46
	Salt water	15	521.184	35.06	6.73	103.51	7.594	2.40	31.62	23.05
		90	476.825	59.57	12.49	94.70	7.687	2.01	26.17	22.20
		180	472.098	70.66	14.97	93.76	7.343	2.49	33.92	25.62
		360	385.034	124.48	32.33	76.47	6.475	3.22	49.77	34.46
	Salt fog	15	507.792	48.45	9.54	100.85	9.113	0.88	9.66	7.69
		90	484.285	52.11	10.76	96.18	8.806	0.89	10.11	10.86
		180	476.576	66.18	13.89	94.65	6.787	3.05	44.99	31.27
		360	429.046	80.47	18.76	85.21	5.907	3.79	64.23	40.22
	Combined hydrothermal condition	15	472.645	83.60	17.69	93.87	8.698	1.3	14.96	11.90
		90	447.573	88.82	19.84	88.89	7.169	2.53	35.34	27.42
		180	442.805	119.95	28.37	83.97	6.441	3.39	52.64	34.80
		360	400.444	109.07	27.24	79.53	5.232	4.46	85.28	47.03
	Sustained load	15	447.574	108.67	24.28	88.89	8.505	1.49	17.53	13.93
		90	430.202	106.19	24.68	85.44	6.948	2.72	39.19	29.67
		180	398.387	144.37	36.24	79.12	6.062	3.77	62.21	38.63
		360	380.107	129.41	34.05	75.49	4.988	4.71	94.58	49.59
VE			Unexposed tensile strength = 531.712 (MPa); Unexposed elastic modulus = 11.693 (GPa)							
	Deionized water	15	549.736	-5.77	-1.05	103.39	12.676	-0.53	-4.18	-8.37
		90	596.699	-65.08	-10.91	110.34	11.714	-0.34	-2.90	-0.20
		180	494.286	25.83	5.23	92.96	10.402	1.09	10.48	11.04
		360	442.171	66.68	15.08	83.16	9.012	2.78	30.85	22.95
	Salt water	15	568.724	-24.76	-4.35	106.96	10.979	1.17	10.67	6.13
		90	522.304	9.31	1.78	98.23	11.944	-0.57	-4.77	-2.18
		180	522.307	-2.19	-0.42	98.23	11.256	0.23	2.13	3.77
		360	512.576	-3.72	-0.72	96.40	10.157	1.64	16.16	13.18
	Salt fog	15	558.932	-15.97	-2.86	105.12	12.509	-0.36	-2.88	-6.91
		90	554.203	-22.59	-4.08	104.23	11.677	-0.30	-2.57	0.16
		180	530.336	-10.22	-1.93	99.74	11.339	0.16	1.41	3.05
		360	507.412	1.44	0.28	95.43	10.978	0.82	7.47	6.17
	Combined hydrothermal condition	15	541.289	2.68	0.49	101.80	12.563	-0.42	-3.34	-7.42
		90	538.461	-6.85	-1.27	101.27	13.353	-1.98	-14.83	-14.22
		180	532.084	-11.97	-2.25	100.07	12.667	-1.17	-9.24	-8.28
		360	529.644	-20.79	-3.92	99.61	12.243	-0.45	-3.68	-4.68



amplitude. However, the degrees of T_g increase and decrease of VE profiles are higher than those of UP profiles, indicating that vinyl resin is more sensitive to high temperature and high humidity environments and is subject to drastic changes of environmental factors.

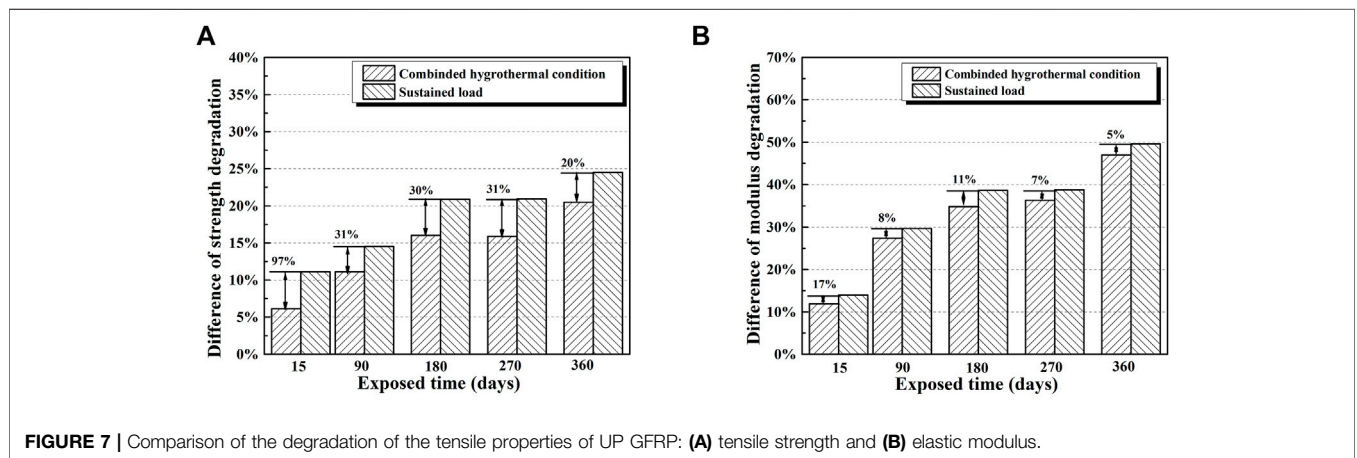
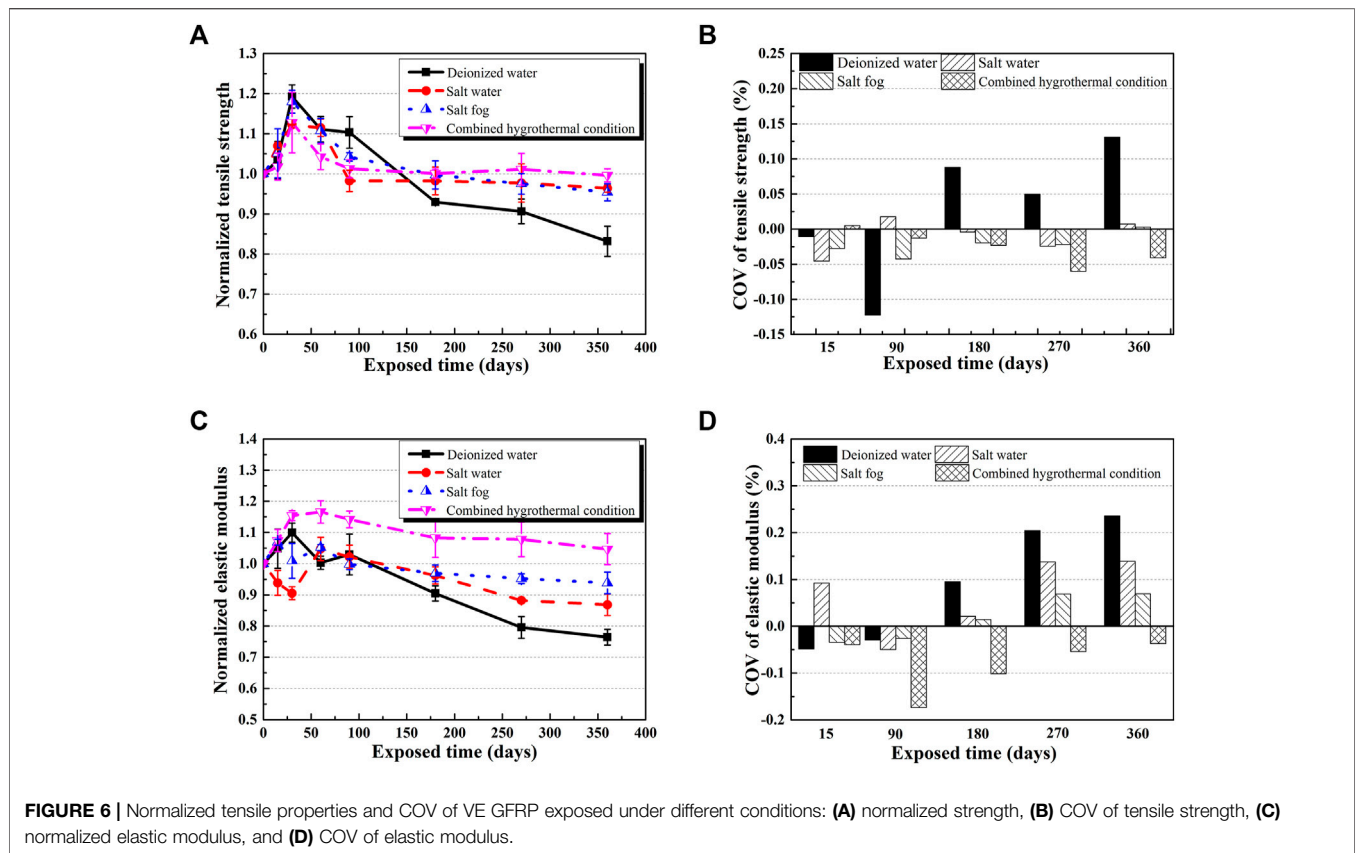
Tensile Characterization

The test results of the tensile properties, including the strength and elastic modulus of GFRP profiles based on UP resin and VE resin exposed in different environments, are summarized in **Table 2**. In general, similar amounts of strength degradation of VE profiles can be found regardless of the aging duration for exposure in all types of environments, except for immersion in deionized water. Moreover, the same pattern of degradation can be observed in the variation of the elastic modulus. The standard deviation (SD) and COVs presented the change range and ratio of the strength and modulus in aging environments and controlled conditions. In contrast, the strength and modulus degradation of the UP profiles exhibited relatively larger amplitudes compared to those of the VE profiles. The results indicated that GFRP profiles had good salt resistance but relatively weak water corrosion resistance. Furthermore, VE resin had more stable erosion resistance than UP resin in hygrothermal environments.

The variations in the residual tensile properties of UP profiles and VE profiles with respect to the exposure time are shown in **Figures 5, 6**, respectively. More intuitive and obvious trends of changes could be observed. Continuing declines are observed in

Figures 5A,C. A change was observed in the UP profiles exposed to the combined hygrothermal cycle condition; the amplitude of descent was almost the highest one of all conditions, and the strength and modulus decreased by 20.47 and 47.03%, respectively. Moreover, the values of the strength variation were 24.03, 23.53, and 14.79% under exposure to deionized water, salt water, and the salt fog cycle conditions, respectively. In particular, the modulus variations were nearly 35% in the deionized water immersion, salt water immersion, and salt fog cycle conditions. In contrast, the tensile strength of the VE profiles exhibited a slight increase (~1.2%), caused by postcuring in the first 30 days, followed by a sharp decline to 98% until 180 days, which was mainly related to random fiber breakage and delamination, before remaining flat at the end of the test (see **Figures 6A,C**). In contrast, for the VE profiles, the strength degraded only 0.39% and the modulus increased 4.68% after 360 combined hygrothermal cycles. Moreover, the worst condition occurred under immersion in deionized water, with 16.84 and 22.95% degradations in the tensile strength and modulus, respectively. Inignorably, an initial increase of tensile properties could be observed under all conditions. It was highly possibly caused by the post curing. The results indicated that the effects of temperature and water absorption on UP resin were more obvious than those on VE resin, thus proving the good corrosion resistance of VE resin.

As shown in **Figures 5B,D**, higher COVs were observed for the exposed UP-based GFRP profiles than for the control UP-



based GFRP profiles. Liu et al. (2020) attributed this trend to nonuniformity in the concentration of microcracking in the exposed composites. The tensile strength of GFRP profiles had higher COV values than the modulus after exposure, indicating that the strength of GFRP composites was more sensitive to temperature and moisture than the modulus. As shown in **Figures 6B,D**, the COVs of the VE-based GFRP profiles were small, except for under immersion in deionized water, and some of them were less than zero. In other words, no significant and continuous fiber fracture or interface debonding occurred on the

VE-based GFRP profiles, and the degree of postcuring of the material even deepened. Thus, there was a slight increase or decrease in strength and modulus.

The combined hygrothermal condition has the most profound negative effects on the tensile properties of pultruded UP profiles; therefore, the sustained loading factor was added in this condition. **Figure 7** presents the difference in the tensile property reductions of UP profiles induced by pure corrosion and the prestressing effect. The test data are also shown in **Table 2**. The contribution of

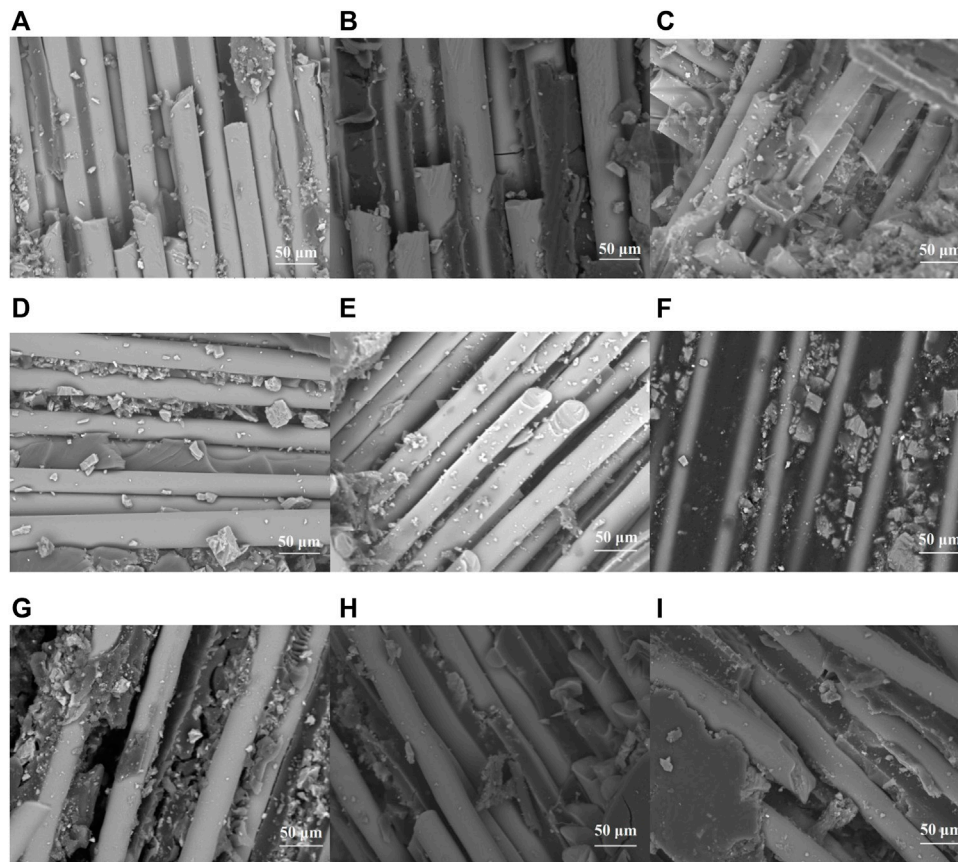


FIGURE 8 | Scanning electron micrographs of the UP GFRP specimens: **(A)** unexposed, **(B)** exposed to deionized water for 30 days, **(C)** exposed to deionized water for 360 days, **(D)** exposed to salt water for 30 days, **(E)** exposed to salt water for 360 days, **(F)** exposed to salt fog for 30 days, **(G)** exposed to salt fog for 360 days, **(H)** exposed to combined hygrothermal cycling without sustained loading for 30 days, and **(I)** exposed to combined hygrothermal cycling without sustained loading for 360 days.

sustained loading to the degradation of the mechanical properties can be clearly observed. For tensile strength, because of the sensitive microcracks developed by prestressing and because the samples were not fully cured, the largest difference between the two groups reached 97% in the initial time. Moreover, the amplitude of the strength degradation induced by the combined hygrothermal condition with sustained loading at 15 days of aging was the same as the amplitude of degradation by pure corrosion at 30 days of aging. Out of expectation, the sustained loading can barely improve the curing rate and accelerate the degradation rate of the UP profiles under combined hygrothermal cycles. As shown in **Figure 7B**, the acceleration effect of prestressing on modulus degradation was similar to the amount of degradation directly induced by corrosive elements. After 15 days of aging, the maximum difference between modulus degradations of UP GFRP profiles with or without sustained loading is 17%, and the minimum difference is 5%, measured at 360 days of aging. The results showed that the influence of prestressing on tensile properties was more

significant in the early stage of aging and then weakened with increasing aging time.

Morphology Analysis

To determine whether the aging conditions caused any physical damage to GFRP profiles, the microstructures of GFRP profiles from different environments were observed using SEM measurements. Because there are more severe damages of UP profiles on the tensile properties than those of VE profiles spotted in different environments, UP profiles were chosen on for the microstructure observetily. **Figure 8A** presents the microstructure of the control specimen, which showed strong adhesion between the fiber and matrix without significant fiber pull-out or uneven matrix fragments, as well as smooth fiber surfaces. The adhesion behavior between the fiber and the matrix plays an important role in the loading transfer from the matrix to the fiber. **Figures 8B–I** show the surfaces of the specimens aged in deionized water, salt water, salt fog cycles, and combined hygrothermal cycles without sustained loading for 30 and 360 days. Compared with **Figure 8B**, the surface of the fiber

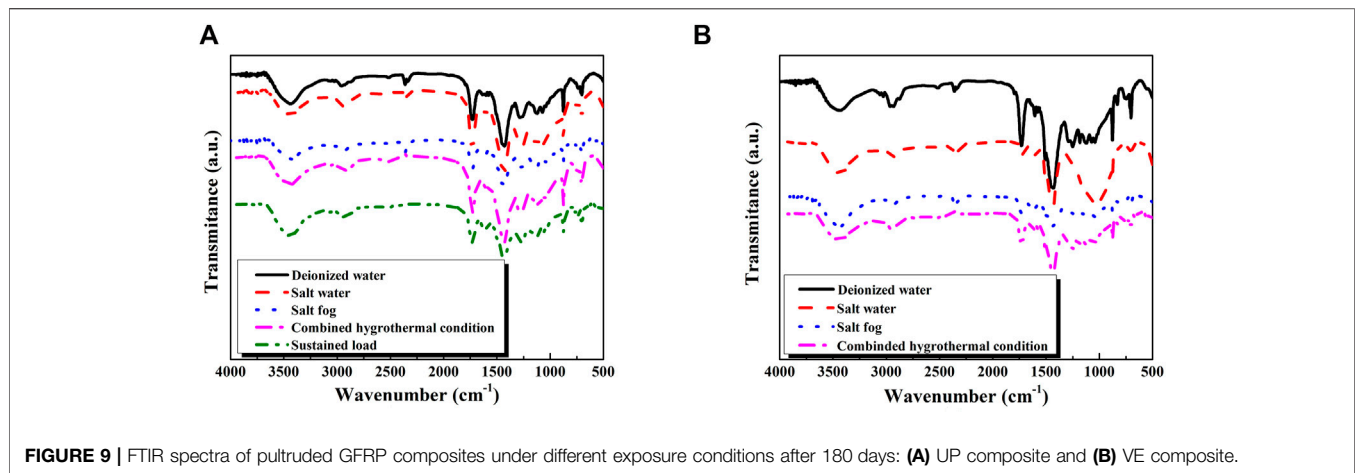


FIGURE 9 | FTIR spectra of pultruded GFRP composites under different exposure conditions after 180 days: **(A)** UP composite and **(B)** VE composite.

TABLE 3 | Functional group changes of GFRP composites after environmental exposure.

Environment		3421 cm ⁻¹	2956 cm ⁻¹	1731 cm ⁻¹	1436 cm ⁻¹	1089 cm ⁻¹
UP	Deionized water	2.04	-0.91	1.08	0.97	-0.77
	Salt water	1.72	-0.87	1.38	1.17	-0.54
	Salt fog	1.37	-0.91	-0.33	-0.37	-0.83
	Combined hydrothermal condition	1.90	-0.86	1.33	1.00	-0.74
	Sustained load	2.11	-0.89	-0.08	-0.41	-0.81
VE	Deionized water	1.00	-0.81	1.95	1.4	-0.25
	Salt water	1.02	-0.91	-0.56	-0.02	1.87
	Salt fog	-0.02	-0.94	-0.50	-0.63	-1.29
	Combined hydrothermal condition	-0.11	-0.89	1.03	-0.18	-0.56

became rough in **Figure 8C** because of damage caused by hydrolysis and the adsorption of many impurities (e.g., resin particles and water). Resin hydrolysis was the major reason for the degradation of tensile properties for GFRP profiles. **Figures 8D,E** show that the impact of salt on degradation was less obvious than that of water. **Figures 8F,G** show that debonding occurred between the fiber and matrix and microcracks formed in the matrix because of the difference between coefficients of thermal expansion of the fiber and matrix resin. Moreover, fiber pull-out was found in **Figure 8I** compared to **Figure 8H**. Overall, fiber breakage, debonding between the fiber and resin, and a higher degree of polymeric deterioration occurred with increasing exposure time.

Fourier Transform Infrared Spectroscopy Analysis

Figure 9 shows FTIR spectra of UP and VE profiles aged under different conditions after 360 days. In general, the chemical changes are revealed by the changes in the intensity and shape of certain peaks. Certain types of chemical bonds are usually considered in research on the durability of composites, including OH stretch (3421 cm⁻¹), C-H stretch (2956 cm⁻¹), C=O stretch (1731 cm⁻¹), and COOR stretch (1089 cm⁻¹) (Mourad et al., 2010; Salim et al., 2020). The change in the relative peak intensity of the hydroxyl group before and after

aging provided insight into the extent of the hydrolysis reaction of the sample, the peak intensity change in carbon-hydrogen was assumed to correspond to the reaction of the aromatic group, and conjugated double bonds could explain the color change observed on the material surface. **Table 3** shows the normalization of the functional group changes of UP profiles and VE profiles, respectively, after aging based on the intensity of the absorption peak of controlled specimens. The typical peak in **Figure 9A** shows that the maximum value (2.11) of the relative peak intensity of the OH group occurred under the condition of combined hydrothermal cycles with a sustained load, followed by exposure to deionized water (2.04), combined hydrothermal cycles (1.90), salt water immersion (1.72), and salt fog cycles (1.37). Furthermore, the relative peak intensity of the COOR group decreased in the order of the increase in the relative peak intensity of the OH group. These findings suggested that hydrolysis occurred more violently under the hydrothermal conditions; moreover, the process of hydrolysis might be hindered by the presence of salt or catalyzed by sustained loading. The change trend of stretching at 1731 cm⁻¹ was inconspicuous. The C-H group and C=C group showed superficial distinctions between the various conditions; thus, the aromatic group and color were likely not changed significantly. The changes in the peak intensity variations of the OH group and COOR group under different

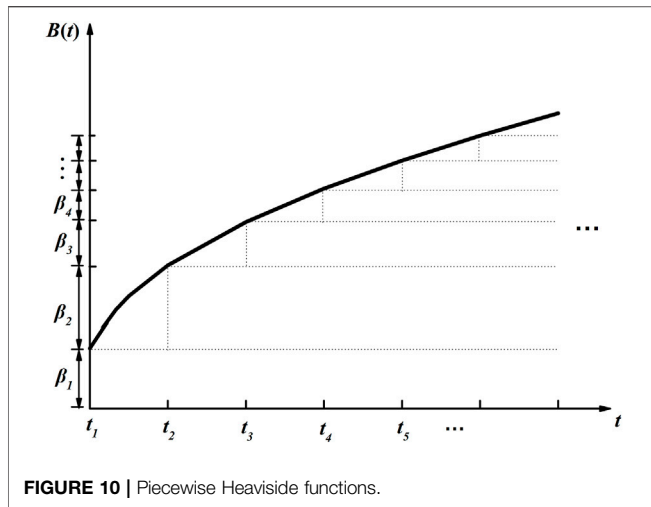


FIGURE 10 | Piecewise Heaviside functions.

conditions were small and had no clear pattern in **Figure 9B**; however, changes in the form of the peaks at 1431 cm^{-1} were observed under the different conditions. These changes in the form can be attributed to the stretching vibration of the aliphatic acid $\nu(\text{CO})$ and the bending vibration of the primary alcohol $\delta(\text{OH})$ (Amaro et al., 2011). The differences in the FTIR spectra between **Figures 9A,B** can be attributed to the different structural formulas of UP resin and VE resin. Thus, the hydrolysis reaction and dehydration reaction following hydrolysis were the main reasons for the degradation of the pultruded GFRP profiles. Furthermore, the conclusions from the FTIR spectra were consistent with the results from the tensile tests.

Damage Model for Glass-Fiber-Reinforced Polymer Profiles Exposed to Combined Hygrothermal Conditions

To study the influence of sustained loading on pultruded GFRP profiles exposed to combined hygrothermal conditions, a damage model with the main elements of aging time, corrosive medium, and loading should be established based on mechanical experiments. Based on the residual strength formula proven by Gunyaev G.M. (Bulmanis et al., 1991), the environment factor has both a positive effect (enhancement process) and a negative effect (damage process) on material performance during aging. Thus, the residual strength equation is given by

$$S = S_0 + \eta(1 - e^{-\lambda t}) - \beta \ln(1 + \theta t) \tag{3}$$

where S is the residual strength of GFRP profiles after t days of aging, S_0 is the initial strength, η is the postcure material parameter, β is the material parameter for resistance to crack propagation (usually a material-specific constant), and λ and θ are material status parameters representing the influence of the environment. In addition, $\eta(1 - e^{-\lambda t})$ and $\beta \ln(1 + \theta t)$ express the enhancement and damage processes, respectively.

However, this equation ignored the memory effect of the material and can only consider the influence of a single environment influence factor on the materials. Therefore, the time-dependent material parameter $B(t)$ and the effect of stress were introduced. Assuming that parameter $B(t)$ can be expressed in the form of piecewise linear, as shown in **Figure 10**, we obtain

$$B(t) = \beta_0 + \alpha t^{1/2}, \beta_1 = B(0) \tag{4}$$

$$\beta_i = B(t_i) - B(t_{i-1}), i = 2, 3, \dots n \tag{5}$$

To consider the effects of stress, fracture mechanics theory can be used to mimic the crack growth of GFRP profiles. According to the literature (Saini et al., 2016), the effects of a specific stress level, temperature, and humidity on the crack velocity V can be described as

$$V = Ke^{(\frac{K}{RT})} \tag{6}$$

where K and b are constants, R is the gas constant, T is the thermodynamic temperature, and C is the stress intensity factor.

For GFRP profiles, several types of damage may exist at once or may be different during different periods. By introducing the stress impact factor assumed for the definition of the cumulative damage model, the damage model can be expressed as

$$\Delta D(i) = A \ln[1 + \beta_i \Gamma(x_i)] \exp(C\sigma), i = 1, 2, \dots \tag{7}$$

where ΔD_i is the damage caused by the i -th day of aging. A is the significant parameter of a specific performance under the aging factor x_i , $\Gamma(x_i)$ is the equivalent aging time for the aging factor (Liu et al., 2013) and can be expressed as

$$\Gamma(x_i) = \frac{\text{intensity} \times \text{time}}{\text{benchmark}} \tag{8}$$

Hence, the cumulative damage model can be expressed as follows:

$$D_i = \sum_{i=1}^t \Delta D_i \tag{9}$$

where D_i is the accumulated damage up to the i th day of aging.

When the aging time is equal to the fatigue life t , **Eq. 9** can be written as

$$D(t) = A \exp(C\sigma) \sum_{i=1}^t \ln[1 + \beta_i \Gamma(x_i)] \tag{10}$$

Substituting **Eqs. 4, 5, 10** into **Eq. 3** yields

TABLE 4 | Equivalent data.

Durations (days)	0	15	30	60	90	180	270	360
$\Gamma(x)$	0	26.1	52.2	104.4	156.6	313.2	469.8	626.4
$\Gamma(y)$	0	21.7	43.5	87	130.5	261	391.5	522

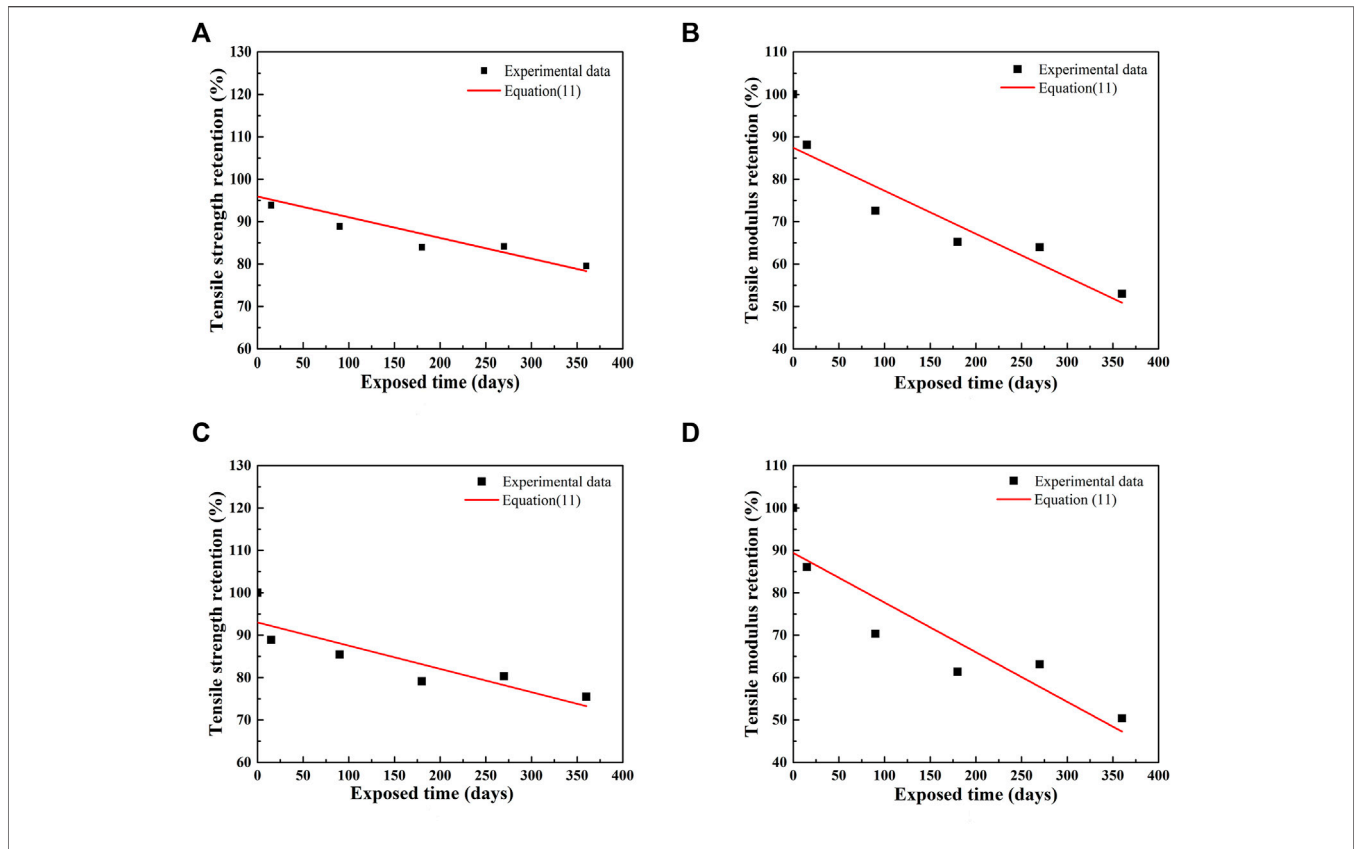


FIGURE 11 | Comparison of the prediction of (A) tensile strength of pultruded UP GFRP profiles under the combined hygrothermal condition, (B) tensile modulus of pultruded UP GFRP profiles under the combined hygrothermal condition, (C) tensile strength of pultruded UP GFRP profiles under the combined hygrothermal condition with sustained loading, and (D) tensile modulus of pultruded UP GFRP profiles under the combined hygrothermal condition with sustained loading.

TABLE 5 | Predictive equations for tensile properties under combined hygrothermal conditions based on Eq. 11.

Properties	Load level (%)	Equation	R-square
strength	0	$94.73 - 0.09 \times \{ \sum \ln [1 + 0.46 \times (t_i^{0.5} - t_{i-1}^{0.5}) \times 1.74t_i] + \sum \ln [1 + 0.36 \times (t_i^{0.5} - t_{i-1}^{0.5}) \times 1.45t_i] \}$	0.87
	40	$93.02 - 0.09 \times \exp(0.39\sigma) \times \{ \sum \ln [1 + 0.57 \times (t_i^{0.5} - t_{i-1}^{0.5}) \times 1.74t_i] + \sum \ln [1 + 0.54 \times (t_i^{0.5} - t_{i-1}^{0.5}) \times 1.45t_i] \}$	0.81
Elastic modulus	0	$87.45 - 0.21 \times \{ \sum \ln [1 + 0.46 \times (t_i^{0.5} - t_{i-1}^{0.5}) \times 1.74t_i] + \sum \ln [1 + 0.36 \times (t_i^{0.5} - t_{i-1}^{0.5}) \times 1.45t_i] \}$	0.78
	40	$89.42 - 0.21 \times \exp(0.35\sigma) \times \{ \sum \ln [1 + 0.68 \times (t_i^{0.5} - t_{i-1}^{0.5}) \times 1.74t_i] + \sum \ln [1 + 0.22 \times (t_i^{0.5} - t_{i-1}^{0.5}) \times 1.45t_i] \}$	0.85

$$S(t) = S_0 + \eta(1 - e^{-\lambda t}) - A \cdot \exp(C\sigma) \left[\sum_{i=1}^t \ln [1 + \beta_{1i} \cdot \Gamma(x_i)] + \sum_{i=1}^t \ln [1 + \beta_{2i} \cdot \Gamma(y_i)] \right],$$

$i = 1, 2, 3, \dots$

(11)

where $\Gamma(x_i)$ is the equivalent time under the influence of temperature and $\Gamma(y_i)$ is the equivalent time under the influence of humidity; they are defined as

$$\Gamma(x_i) = \frac{\bar{T}}{23^\circ\text{C}} \cdot i = 1.74i \tag{12}$$

$$\Gamma(y_i) = \frac{\bar{H}}{65\%} \cdot i = 1.45i \tag{13}$$

Where \bar{T} is the average temperature of exposed conditions per day, \bar{H} is the average humidity of exposed conditions per day, and i is the aging time. The temperature and humidity under controlled conditions are defined as 23°C and 65%, respectively. The data of $\Gamma(x_i)$ and $\Gamma(y_i)$ are shown in Table 4.

Through MATLAB software, Eq. 11 is used to analyze the tensile strength and elastic modulus data according to the experiment data given in Table 2. The predictive result is shown in Figure 11 and Table 5. Given the difference in load conditions (with or without load), most of the fitting curves match the experiment results reasonably well. Whether the stress

exists or not, the parameter A has the same value. For the tensile strength, the value of A is 0.09, and for the tensile modulus, the value of A is 0.21. It means that the tensile strength of GFRP profiles has a better environmental corrosion resistance performance than the modulus under the same environment. When the load level is zero, the parameter α keeps the same between the strength and modulus. In addition, α_1 (represents the influence degree of temperature) is 0.46 and α_2 (represents the influence degree of humidity) is 0.36. It is shown that α_1 rises to 0.57 and α_2 rises to 0.54 in fitting curves for tensile strength with 0.4 f_u prestressing ratios, and the negative impacts of both temperature and humidity on the material are deepened. However, in fitting curves for tensile modulus, α_1 rises to 0.68 and α_2 reduces to 0.22. It means that the negative impact of temperature is deepened, but the negative impact of humidity is weakened.

CONCLUSION

In this paper, the hygrothermal durability of GFRP pultruded profiles made of both UP and VE resins with respect to deionized water, salt water, salt fog, combined hygrothermal cycles, and combined hygrothermal cycles with sustained loading for a period of 12 months was investigated and discussed.

To this scope, a large experimental program was developed comprising 360 tensile test samples (five per each condition). The changes of tensile strength, tensile modulus, and microstructure were evaluated with the absorption behavior by evaluating the change in weight of the samples.

- 1) The moisture absorption of both UP and VE profiles increased initially and then leveled off. The VE profiles exhibited a lower mass uptake and faster moisture absorption than the UP profiles. To some extent, the presence of salt prevented the diffusion of water. Moreover, high temperatures can increase the moisture diffusion rate.
- 2) Tensile properties declined according to the moisture absorption of GFRP profiles. Moreover, the VE profile had a more stable erosion resistance than the UP profile in typical hygrothermal environments. Moreover, the modulus was more affected than tensile strength under all conditions, especially at high temperatures.
- 3) Sustained loading did not change the trend of the degradation in tensile properties but increased the rate and amplitude of degradation. Prestressing accelerated the development of microcracks and gaps.
- 4) The abovementioned degradation mainly occurred because of physical degradation phenomena, namely, plasticization of the polymeric matrix as well as the fiber breakage and debonding between the fiber and resin, as seen in the SEM images, with little

appreciable chemical degradation, that is, hydrolysis, observed in the FTIR analysis. With the obvious decrease in the relative peak intensity of the COOR group and the increase in the relative peak intensity of the OH group, hydrolysis occurred violently in the UP profiles. In contrast, the chemical groups had no apparent change for the VE profiles.

- 5) The accumulative damage model of the semiempirical and semitheoretical analysis provided a method to predict the residual tensile properties of pultruded GFRP profiles exposed to a combined hygrothermal condition with sustained load. It showed that environmental factors can cause a large decline in tensile modulus relative to tensile strength. Moreover, temperature had a more serious influence on properties than humidity.

DATA AVAILABILITY STATEMENT

The raw data supporting the conclusions of this article will be made available by the authors, without undue reservation.

AUTHOR CONTRIBUTIONS

Conceptualization, SY; methodology, SY; micrographs, YL and ZX; investigation, SY, MC, and FC; data curation, MF; writing—original draft preparation, SY; writing—review and editing, NF and MC; visualization, SY, FC, and MF; supervision, YS and JL.

FUNDING

SY is the moderator of The Major Basic Research Project of the Natural Science Foundation of the Jiangsu Higher Education Institutions of China (No: 21KJB560009), RMB 30000, the PhD Research Startup Foundation of Changzhou Institute of Technology (No: E3620720001), RMB 20000, and The National College Students Innovation and Entrepreneurship Training Program (No: 202111055013Z), RMB 5000; NF is the moderator of the Foundation of Changzhou Sci & Tech Program (No: CE20219002) and the Industry–University Research Cooperation Project of Jiangsu Province (No: BY2021177), RMB 300000; YS is the moderator of the Foundation of Changzhou Sci & Tech Program (No: CJ20210153 and CZ20210032); JL is the moderator of The Major Basic Research Project of the Natural Science Foundation of the Jiangsu Higher Education Institutions of China (No: 21KJD560004), the Foundation of Changzhou Sci & Tech Program (No: CJ20210132).

REFERENCES

- ACI 440.1R-06 (2006). *Guide for the Design and Construction of Structural Concrete Reinforced with FRP Bars*. Farmington Hills, Michigan: American Concrete Institute.
- ACI 440.2R-08 (2008). *Guide for the Design and Construction of Externally FRP Systems for Strengthening Concrete Structures*. Farmington Hills, Michigan: American Concrete Institute.
- Amaro, A. M., Reis, P. N. B., and de Moura, M. F. S. F. (2011). Delamination Effect on Bending Behaviour in Carbon-Epoxy Composites. *Strain* 47 (2), 203–208. doi:10.1111/j.1475-1305.2008.00520.x
- ASTM D3039/D3039M-14 (2014). *Standard Test Method for Tensile Properties of Polymer Matrix Composite Materials*. West Conshohocken, PA: ASTM International.
- ASTM D5229/D5229M (2014). *Standard Test Method for Moisture Absorption Properties and Equilibrium Conditioning of Polymer Matrix Composite Materials*. West Conshohocken, PA: ASTM International.
- Bulmanis, V. N., Gunyaev, G. M., and Krivosos, V. V. (1991). “In-Service Durability Prediction of Structural CFRP,” in *The MICC 90*. Editors I. N. Fridlyander and V. I. Kostikov (Dordrecht: Springer), 1254–1257. doi:10.1007/978-94-011-3676-1_241
- Carra, G., and Carvelli, V. (2014). Ageing of Pultruded Glass Fibre Reinforced Polymer Composites Exposed to Combined Environmental Agents. *Compos. Structures* 108 (1), 1019–1026. doi:10.1016/j.compstruct.2013.10.042
- Chin, J. W., Nguyen, T., and Aouadi, K. (1999). Sorption and Diffusion of Water, Salt Water, and concrete Pore Solution in Composite Matrices. *J. Appl. Polym. Sci.* 71, 483–492. doi:10.1002/(sici)1097-4628(19990118)71:3<483:aid-app15>3.0.co;2-s
- Dell’Anno, G., and Lees, R. (2012). Effect of Water Immersion on the Interlaminar and Flexural Performance of Low Cost Liquid Resin Infused Carbon Fabric Composites. *Compos. Part. B* 43 (3), 1368–1373. doi:10.1016/j.compositesb.2011.08.037
- Duo, Y., Liu, X., Liu, Y., Tafsirojjaman, T., and Sabbrojjaman, M. (2021). Environmental Impact on the Durability of FRP Reinforcing Bars. *J. Building Eng.* 43, 102909. doi:10.1016/j.jobbe.2021.102909
- Fang, Y., Wang, K., Hui, D., Xu, F., Liu, W., Yang, S., et al. (2017). Monitoring of Seawater Immersion Degradation in Glass Fibre Reinforced Polymer Composites Using Quantum Dots. *Composites B: Eng.* 112, 93–102. doi:10.1016/j.compositesb.2016.12.043
- Feng, P., Wang, J., Wang, Y., Loughery, D., and Niu, D. (2014). Effects of Corrosive Environments on Properties of Pultruded GFRP Plates. *Composites Part B: Eng.* 67, 427–433. doi:10.1016/j.compositesb.2014.08.021
- Gribniak, V., Rimkus, A., Plioplys, L., Misiūnaitė, I., Garnevičius, M., Boris, R., et al. (2021). An Efficient Approach to Describe the Fiber Effect on Mechanical Performance of Pultruded GFRP Profiles. *Front. Mater.* 8, 746376. doi:10.3389/fmats.2021.746376
- Jiang, X., Kolstein, H., Bijlaard, F., and Qiang, X. (2014). Effects of Hygrothermal Aging on Glass-Fibre Reinforced Polymer Laminates and Adhesive of FRP Composite Bridge: Moisture Diffusion Characteristics. *Composites A: Appl. Sci. Manufacturing* 57 (1), 49–58. doi:10.1016/j.compositesa.2013.11.002
- Kafodya, I., Xian, G., and Li, H. (2015). Durability Study of Pultruded CFRP Plates Immersed in Water and Seawater under Sustained Bending: Water Uptake and Effects on the Mechanical Properties. *Composites Part B: Eng.* 70, 138–148. doi:10.1016/j.compositesb.2014.10.034
- Liu, C. C., Wang, H. W., and Yang, X. H. (2013). Study of Accelerated Corrosion Test Environment Spectrum of Different Materials in marine Atmospheric Environment. *Equipment. Environmental Eng.* 10 (2), 18–24. CNKI:SUN:JSCX.0.2013-02-004.
- Liu, T., Liu, X., and Feng, P. (2020). A Comprehensive Review on Mechanical Properties of Pultruded FRP Composites Subjected to Long-Term Environmental Effects. *Composites Part B: Eng.* 191, 107958. doi:10.1016/j.compositesb.2020.107958
- Liu, X., Li, F., and Wang, X. (2022). Synergistic Effect of Acidic Environmental Exposure and Fatigue Loads on FRP Tendons. *Construction Building Mater.* 314 (3), 125584. doi:10.1016/j.conbuildmat.2021.125584
- Ma, G., Yan, L., Shen, W., Zhu, D., Huang, L., and Kasal, B. (2018). Effects of Water, Alkali Solution and Temperature Ageing on Water Absorption, Morphology and Mechanical Properties of Natural FRP Composites: Plant-Based Jute vs. mineral-based basalt. *Composites Part B: Eng.* 153 (15), 398–412. doi:10.1016/j.compositesb.2018.09.015
- Mancusi, G., Spadea, S., and Berardi, V. P. (2013). Experimental Analysis on the Time-Dependent Bonding of FRP Laminates Under Sustained Loads. *Compos.* 46 (2), 116–122. doi:10.1016/j.compositesb.2012.10.007
- Mourad, A.-H. I., Abdel-Magid, B. M., El-Maaddawy, T., and Grami, M. E. (2010). Effect of Seawater and Warm Environment on Glass/Epoxy and Glass/Polyurethane Composites. *Appl. Compos. Mater.* 17 (5), 557–573. doi:10.1007/s10443-010-9143-1
- Nakada, M., and Miyano, Y. (2014). Effect of Water Absorption on Time-Temperature Dependent Strength of Unidirectional CFRP. *Solid Mech. its Appl.* 208, 155–164. doi:10.1007/978-94-007-7417-9_7
- Qu, F., Li, W., Dong, W., Tam, V. W. Y., and Yu, T. (2021). Durability Deterioration of Concrete under Marine Environment from Material to Structure: A Critical Review. *J. Building Eng.* 35, 102074. doi:10.1016/j.jobbe.2020.102074
- Robert, M., and Fam, A. (2012). Long-Term Performance of GFRP Tubes Filled with Concrete and Subjected to Salt Solution. *J. Compos. Constr.* 16 (2), 217–224. doi:10.1061/(ASCE)CC.1943-5614.0000251
- Saini, A., Chhibber, R., and Chattopadhyay, A. (2016). Effect of Combined Fatigue and Hygrothermal Loading on Structural Properties of E-Glass/Polymers. *Proc. Inst. Mech. Eng. C: J. Mech. Eng. Sci.* 231 (18), 3382–3392. doi:10.1177/0954406216644268
- Salim, M. S., Ariawan, D., AhmadRasyid, M. F., MatTaib, R., AhmadThirmizir, M. Z., and MohdIshak, Z. A. (2020). Accelerated Weathering and Water Absorption Behavior of Kenaf Fiber Reinforced Acrylic Based Polyester Composites. *Front. Mater.* 7, 26. doi:10.3389/fmats.2020.00026
- Scott, P., and Lees, J. M. (2013). Water, Salt Water, and Alkaline Solution Uptake in Epoxy Thin Films. *J. Appl. Polym. Sci.* 130 (3), 1898–1908. doi:10.1002/app.39331
- Sousa, J. M., Garrido, M., Correia, J. R., and Cabral-Fonseca, S. (2021). Hygrothermal Ageing of Pultruded GFRP Profiles: Comparative Study of Unsaturated Polyester and Vinyl Ester Resin Matrices. *Composites Part A: Appl. Sci. Manufacturing* 140, 106193. doi:10.1016/j.compositesa.2020.106193
- Starkova, O., Aniskevich, K., and Sevcenko, J. (2021). Long-Term Moisture Absorption and Durability of FRP Pultruded Rebars. *Mater. Today Proc.* 34 (1), 36–40. doi:10.1016/j.matpr.2019.12.154
- Tu, J., Xie, H., Gao, K., Li, Z., and Zhang, J. (2019). Durability Prediction of GFRP Rebar Based on Elastic Modulus Degradation. *Front. Mater.* 6, 258. doi:10.3389/fmats.2019.00258
- Vizentin, G., and Vukelic, G. (2022). Failure Analysis of FRP Composites Exposed to Real marine Environment. *Proced. Struct. Integrity* 37, 233–240. doi:10.1016/j.prostr.2022.01.079
- Zeng, J.-J., Zhuge, Y., Liang, S.-D., Bai, Y.-L., Liao, J., and Zhang, L. (2022). Durability Assessment of PEN/PET FRP Composites Based on Accelerated Aging in Alkaline Solution/Seawater with Different Temperatures. *Construction Building Mater.* 327, 126992. doi:10.1016/j.conbuildmat.2022.126992

Conflict of Interest: The authors declare that the research was conducted in the absence of any commercial or financial relationships that could be construed as a potential conflict of interest.

Publisher’s Note: All claims expressed in this article are solely those of the authors and do not necessarily represent those of their affiliated organizations or those of the publisher, the editors, and the reviewers. Any product that may be evaluated in this article or claim that may be made by its manufacturer is not guaranteed or endorsed by the publisher.

Copyright © 2022 Yang, Chu, Chen, Fu, Lv, Xiao, Feng, Song and Li. This is an open-access article distributed under the terms of the Creative Commons Attribution License (CC BY). The use, distribution or reproduction in other forums is permitted, provided the original author(s) and the copyright owner(s) are credited and that the original publication in this journal is cited, in accordance with accepted academic practice. No use, distribution or reproduction is permitted which does not comply with these terms.